Bosakova *et al.*
Cell Communication and Signaling (2025) 23:209
https://doi.org/10.1186/s12964-025-02208-w

Cell Communication and Signaling

RESEARCH

Open Access

Endoplasmic reticulum stress disrupts signaling via altered processing of transmembrane receptors

Michaela Bosakova[1,2,3], Sara P. Abraham[1,2,3], Davis Wachtell[4], Jennifer T. Zieba[4], Alexander Kot[4], Alexandru Nita[1,2], Aleksandra Anna Czyrek[1,3], Adolf Koudelka[1], Vlad-Constantin Ursachi[1,3], Zuzana Feketova[1,3], Gustavo Rico-Llanos[1,3], Katerina Svozilova[1,2], Petra Kocerova[1,2], Bohumil Fafilek[1,2,3], Tomas Gregor[1,3], Jana Kotaskova[5], Ivan Duran[4], Petr Vanhara[7], Michael Doubek[5], Jiri Mayer[5], Karel Soucek[3,6,8], Deborah Krakow[4*] and Pavel Krejci[1,2,3*]

Abstract

Cell communication systems based on polypeptide ligands use transmembrane receptors to transmit signals across the plasma membrane. In their biogenesis, receptors depend on the endoplasmic reticulum (ER)-Golgi system for folding, maturation, transport and localization to the cell surface. ER stress, caused by protein overproduction and misfolding, is a well-known pathology in neurodegeneration, cancer and numerous other diseases. How ER stress affects cell communication via transmembrane receptors is largely unknown. In disease models of multiple myeloma, chronic lymphocytic leukemia and osteogenesis imperfecta, we show that ER stress leads to loss of the mature transmembrane receptors FGFR3, ROR1, FGFR1, LRP6, FZD5 and PTH1R at the cell surface, resulting in impaired downstream signaling. This is caused by downregulation of receptor production and increased intracellular retention of immature receptor forms. Reduction of ER stress by treatment of cells with the chemical chaperone tauroursodeoxycholic acid or by expression of the chaperone protein BiP resulted in restoration of receptor maturation and signaling. We show a previously unappreciated pathological effect of ER stress; impaired cellular communication due to altered receptor processing. Our findings have implications for disease mechanisms related to ER stress and are particularly important when receptor-based pharmacological approaches are used for treatment.

Keywords Endoplasmic reticulum, ER, Stress, Receptor, Transmembrane, Signaling, Impaired

*Correspondence:
Deborah Krakow
DKrakow@mednet.ucla.edu
Pavel Krejci
krejcip@med.muni.cz
[1] Department of Biology, Faculty of Medicine, Masaryk University, 62500 Brno, Czech Republic
[2] Institute of Animal Physiology and Genetics, Czech Academy of Sciences, 60200 Brno, Czech Republic
[3] International Clinical Research Center, St. Anne's University Hospital, 65691 Brno, Czech Republic
[4] Department of Orthopaedic Surgery, Human Genetics, and Obstetrics and Gynecology, University of California at Los Angeles, Los Angeles, CA 90095, USA
[5] Department of Internal Medicine, Hematology and Oncology, University Hospital Brno, 62500 Brno, Czech Republic
[6] Department of Experimental Biology, Faculty of Science, Masaryk University, 62500 Brno, Czech Republic
[7] Department of Histology and Embryology, Faculty of Medicine, Masaryk University, 62500 Brno, Czech Republic
[8] Department of Cytokinetics, Institute of Biophysics, Czech Academy of Sciences, 61265 Brno, Czech Republic

Introduction

Most proteins that form the extracellular matrix, proteins destined for the cell surface and proteins that are released from the cell are co-translationally translocated into the lumen of the endoplasmic reticulum (ER) and transported to the cell membrane via the ER-Golgi system. Within the ER, chaperones and enzymes assist in protein folding, post-translational modifications, maturation and transport. Sophisticated ER quality control systems monitor and prevent the aggregation of proteins. Ideally, only properly folded and mature proteins leave the ER. The accumulation of misfolded proteins beyond cellular capacity triggers the unfolded protein response (UPR). In mammalian cells, there are three major ER-resident UPR regulators: IRE1α (inositol-requiring enzyme 1α), PERK (PRKR-like ER kinase) and ATF6 (activating transcription factor 6) (Fig. S1). Under normal conditions, these proteins are inactive at the ER membrane due to binding by the chaperone BiP (binding immunoglobulin protein). When ER stress is triggered, BiP is released from these regulators to help process the accumulating misfolded proteins, leading to IRE1α, PERK and ATF6 activation. This in turn upregulates the expression of other UPR mediators such as XBP1 s (X-box binding protein 1), HERPUD1 (homocysteine-responsive endoplasmic reticulum-resident ubiquitin-like domain member 1), ATF4 or CHOP (C/EBP homologous protein) [1, 2]. The baseline function of the UPR is to maintain ER homeostasis and preserve cell function, which is referred to as homeostatic UPR [3–5]. However, when the ER's ability to fold proteins or its quality control machinery is overwhelmed, the accumulation of misfolded proteins leads to ER stress that impairs cell function and survival.

The most abundant ER client proteins are the components of the extracellular matrix (ECM), which consists of proteoglycans and collagens, fibronectins, elastins, and laminins [6]. Other classes of cell surface molecules are also transported and matured via the ER. These molecules include transmembrane receptors that respond to communication signals delivered by polypeptide growth factors, cytokines, morphogens, hormones and other ligands. Compared to the ECM components, transmembrane receptors are produced in small quantities. For example, approximately 1·6–80 $\times 10^3$ fibroblast growth factor receptor (FGFR) molecules are present at the cell surface, which is 7·5–22 times less than the amount of ECM proteoglycans that function as FGFR coreceptors [7, 8]. In osteoblasts, the expression of ECM components such as *collagen1a1* is extremely high compared to the expression of receptors for the bone growth factors morphogenetic protein (BMP) and transforming growth factor β (TGFβ) [9]. Similarly, in cartilage, the relative expression of ECM components is significantly higher compared to FGF, TGFβ/BMP and integrin receptors. An example of this is *FGFR3*, which is expressed >100-fold less than *collagen2a1*.[10] In addition, membrane receptors are often unstable proteins that are highly dependent on folding [11], leading to the hypothesis that receptor biogenesis may be very sensitive to changes in the general state of the ER. This is suggested by studies in developing mouse embryos in which induction of transient ER stress by hypoxia leads to loss of FGFR1 signaling in cardiac progenitors, resulting in congenital heart defects due to aberrant morphogenesis [12].

ER stress has been well studied in numerous pathological processes such as neurodegeneration, cancer, inflammation and diabetes (> 25,000 citations in PubMed), identifying key molecules involved in this process [13–17]. In contrast, the effect of ER stress on transmembrane receptors has not yet been established, but emerging evidence suggests that receptor biogenesis is sensitive to ER conditions due to limited receptor expression and high folding requirements. In this study, we investigated how ER stress affects transmembrane receptor signaling. In three disease models characterized by the presence of endogenous ER stress, multiple myeloma, chronic lymphocytic leukemia and osteogenesis imperfecta, we show that ER stress leads to the loss of key mature receptors normally present at the cell surface. This impairs the cell's ability to respond to extracellular stimuli, disrupts downstream cell signaling and contributes to cell pathology through changes in the signaling milieu. Our findings have far-reaching implications for diseases associated with ER stress, as many treatments depend on sufficiently available receptors, and add a previously unappreciated dysfunctional cellular mechanism as a consequence of ER stress.

Results

ER stress impairs FGFR3 maturation in multiple myeloma (MM) cells

MM is a frequently diagnosed hematologic malignancy characterized by an accumulation of terminally differentiated plasma cells [18]. A defining feature of plasma cells is their extensively developed rough ER, necessary for the production and secretion of thousands of antibody molecules per second [19]. Due to this secretory load, MM cells are probably operating at the maximum limit of the adaptive UPR. A mainstay of MM treatment is bortezomib (Bz), a 26S proteosome inhibitor that induces ER stress and causes apoptosis in MM cells [20, 21]. Although the mechanisms underlying MM are complex, a molecular finding in 15% of patients is the markedly increased expression of FGFR3 as a result of a t(4;14)(p16.3;q32) translocation [22].

We hypothesized that induction of ER stress affects FGFR3 trafficking. FGFR3-expressing MM cells KMS11 and KMS18 [23] were treated with three well-defined chemical inducers of the UPR: tunicamycin (Tu), which inhibits N-linked glycosylation by preventing the attachment of oligosaccharides to proteins, thereby blocking protein folding and transit through the ER [24]; brefeldin A (Br), which inhibits ER-Golgi protein transport by disrupting the association of the COP-I coat to the Golgi membrane [25]; and thapsigargin (Tg), which inhibits an ER Ca^{2+}-dependent ATPase, thereby depleting ER Ca^{2+} stores and thus reducing the activity of calcium-dependent chaperones [26]. The extent of ER stress was determined by western blot analyses of the expression of the UPR markers BiP, CHOP, IRE1α, XBP1s, ATF6, PERK, ATF4, and HERPUD1 [27] (Figs. S1, S2). Because induction of ER stress can lead to cellular toxicity, we determined the effect of Tu, Br, and Tg on cell proliferation of KMS11 and KMS18 to identify doses that induce toxic ER stress (Figs. S2A, B). Treatment with non-toxic doses of Tu, Br and Tg resulted in downregulation of the mature FGFR3 isoform and a partial loss of FGFR3 at the cell surface, as detected by western blot and FGFR3 flow cytometry on live KMS11 and KMS18 cells (Figs. 1A, B; S3A, B; S4A). Similarly, Bz downregulated FGFR3 expression and caused a loss of FGFR3 at the cell surface. Treatment of KMS11 and KMS18 cells with the cognate FGFR3 ligand FGF2 resulted in activation of the ERK MAP kinase signaling pathway; ERK activation was lost in cells treated with Tu, Br, Tg, and Bz (Figs. 1C; S3C; S4B). This suggests that ER stress downregulated mature FGFR3 and reduced its downstream signaling.

To gain more insight into the effect of ER stress on FGFR3, 293T cells (Fig. S5) were transfected with human FGFR3 and treated with non-toxic doses of Tu, Br and Tg for 24 h. Mature FGFR3 migrated as a 128·3 kDa protein in SDS-PAGE gels (Fig. 1D) (Table S1); two additional isoforms of 118·6 and 107·6 kDa were detected, representing immature FGFR3. The differences in size are largely due to glycosylation, as shown in cell lysates treated with N-glycosidase F, which caused a ~ 17 kDa downshift on mature FGFR3 migration (Fig. 1E; 111·1 kDa FGFR3). Tu, Br and Tg produced different effects on FGFR3 maturation. The mature 128·3 kDa FGFR3 was lost in Tu- and Br-treated cells in favor of the immature 107·6 kDa and 118·6 kDa variants, respectively. In Tg-treated cells, the production of all FGFR3 variants was downregulated, but the cells still expressed some amount of mature FGFR3 (Fig. 1D). The presence of FGFR3 on the cell surface was examined by flow cytometry in live cells. A statistically significant loss of cell surface FGFR3 was detected in cells treated with Tu and Br, but not in the cells treated with Tg (Fig. 1F). These data are consistent with the western blot analyses of FGFR3 expression (Fig. 1D) and indicate that induction of ER stress by Tu and Br leads to intracellular retention of FGFR3.

To test whether the ER stress effect on FGFR3 migration is not due to de novo biogenesis after transfection, we analyzed Tu, Br and Tg effect on endogenously expressed FGFR3. We were unable to detect endogenous FGFR3 in cultured cells due to its low expression. Therefore, we used CRISPR-Cas9 to introduce the 3xFlag epitope into the *Fgfr3* locus in rat chondrosarcoma cells (RCS-F@F3 cells) (Table S2) and detected endogenous FGFR3 by Flag western blot (Fig. S6). Treatment with Tu resulted in the accumulation of immature 107·3 kDa FGFR3, while Tg strongly downregulated the expression of all FGFR3 variants; RCS-F@F3 cells were found to be resistant to Br, as the downregulation of FGFR3 expression only occurred in cells treated with a near-toxic

(See figure on next page.)

Fig. 1 ER stress impairs FGFR3 maturation and signaling in multiple myeloma cells. **A** Expression of endogenous FGFR3 in KMS11 cells treated with tunicamycin (Tu), brefeldin (Br), thapsigargin (Tg), and bortezomib (Bz), determined by FGFR3 western blot (black arrowhead, mature FGFR3 at the cell surface; open arrowheads, immature FGFR3). Actin served as a loading control. Black, no ER stress; green, non-toxic ER stress; red, toxic ER stress (not determined for Bz). **B** Surface expression of FGFR3 in KMS11 cells, determined by flow-cytometry with FGFR3-PE antibody on live cells. The median intensity values were obtained and normalized to non-treated control. **C** The ERK MAP kinase phosphorylation (p) in KMS11 cells treated with 25–40 ng/ml FGF2 for 30 min. **D** 293T cells were transfected with human FGFR3, and treated with Tu, Br and Tg for 24 h to induce ER stress. **E** The molecular weight of mature FGFR3 is 128·3 kDa, due to glycosylation of immature, 107·6 kDa FGFR3, as evidenced in 293T cell lysates treated with N-glycosidase F (PNGase F). An additional FGFR3 variant (85·8 kDa), corresponding to 853 amino acids of transgenic FGFR3 is observed after longer exposition of the blot. PNGase F-treated cell lysates were diluted to obtain FGFR3 amounts similar to cells treated with 1 µM Tu (actin blot, arrow). **F** Analyses of cell-surface expression of transfected FGFR3 in live 293T cells by flow-cytometry; data were expressed as the relative amount of cell-surface FGFR3 positive cells. **G**, **H** Cell-surface expression of transfected FGFR3 by immunocytochemistry on fixed, non-permeabilized RCS cells (left two panels), or cells permeabilized by Triton-X100 (dashed line, right panel). The graph shows the relative amounts of cells with surface FGFR3 signal. Note the intracellular retention of FGFR3 in RCS cells treated with Tu (arrowheads, versus arrows for cell surface FGFR3). DsRed co-transfection was used to track the FGFR3-transfected cells. **I**, **J** 293T-FGFR3 cells were treated with APY-29 (agonist of the IRE1α endonuclease activity) or KIRA6 (inhibitor of IRE1α kinase activity), and analyzed for FGFR3 expression by western blot. Statistical significances were calculated using Student´s *t*-test ($p < 0{\cdot}05$; ** $p < 0{\cdot}01$, *** $p < 0{\cdot}001$); n.s. – not significant. Bar plots – mean ± S.E. n, number of independent experiments

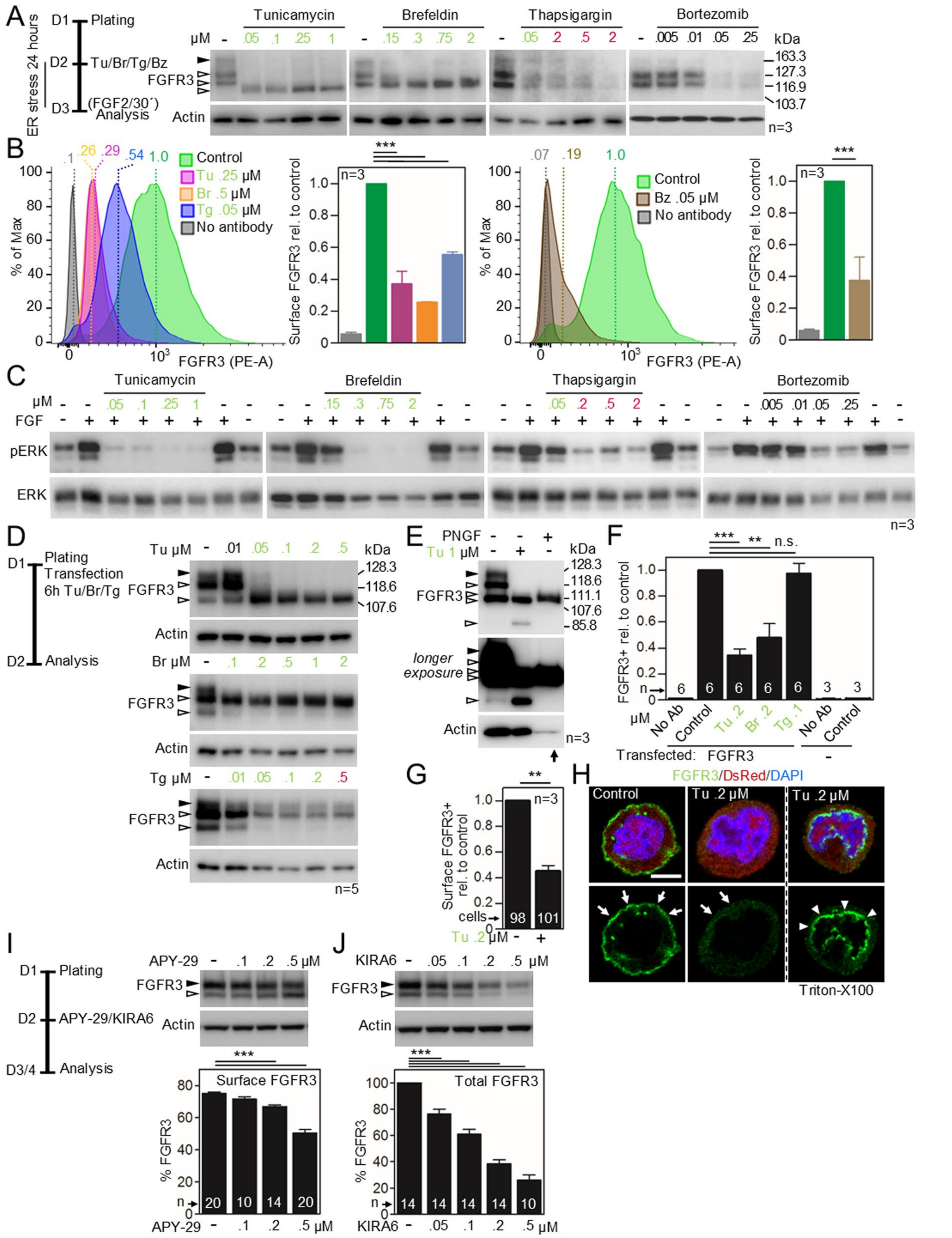

Fig. 1 (See legend on previous page.)

concentration of Br (Fig. S7). Similar to 293T cells, the loss of FGFR3 at the cell surface was also due to intracellular retention, as demonstrated by FGFR3 immunocytochemistry of RCS cells treated with Tu (Fig. 1G, H). Taken together, we found that ER stress diminished cell surface FGFR3 which inhibited the FGF ligand-mediated signaling response.

Next, we modulated the activity of individual ER stress sensors (IRE1α, PERK and ATF6) by a total of six specific chemical inhibitors (Fig. S8) and determined the effect on FGFR3 biogenesis. APY-29 mimics the UPR by inhibiting IRE1α phosphorylation and activating IRE1α ribonuclease function [28]. In 293T cells stably expressing FGFR3 (293T-FGFR3; Table S2), treatment with APY-29 resulted in downregulation of FGFR3 from the cell surface (Fig. 1I). KIRA6 is another modulator of IRE1α which inhibits IRE1α cytoplasmic kinase activity [29]; treatment with KIRA6 inhibited the expression of all FGFR3 variants (Fig. 1J). Modulation of PERK and ATF6 activity by both agonists and antagonists had no effect on FGFR3 biogenesis (Fig. S9). Our data suggest that *FGFR3* transcript is sensitive to UPR-mediated RNA decay (IRE1α endonuclease activity) and that FGFR3 maturation requires IRE1α kinase activity.

ER stress and FGFR1 maturation

We next asked whether ER stress negatively impacted the maturation of fibroblast growth factor receptor 1 (FGFR1) tyrosine kinase with resultant decreased signaling through this receptor, again due to its role in human diseases. Human osteosarcoma U2OS cells stably expressing the BirA-HA-tagged human FGFR1 (U2OS-FGFR1)[30] were treated with Tu, Br, or Tg for 24 h to induce short-term ER stress (Figs. 2A, S10A-C). Cells were analyzed for FGFR1 expression by western blot analyses. The molecular weight of mature, fully glycosylated FGFR1-Bir-HA is approximately 165.5 kDa (Fig. 2A, Table S1). ER stress induced by Tu and Br led to decreased levels of mature FGFR1 protein with a lesser effect induced by Tg. This was confirmed by FGFR1 flow-cytometry on live cells, which showed a decrease of cell surface FGFR1 in cells treated by Tu and Br, but not Tg (Fig. 2B). The FGFR1 immunocytochemistry in Tu-treated cells showed near absence of cell surface FGFR1 with retention of the receptor in the ER, as evidence by immunostaining for ER protein calnexin (Fig. 2C).

Loss of membrane FGFR1 may lead to decreased FGF ligand binding on the cell surface. Imaging of cells treated with recombinant, Cy3-labeled FGF2 showed decreased association of Cy3-FGF2 on the cell surface (Fig. 2D), and was further supported by quantification of cell-associated FGF2 by western blot which showed significantly lower signal in Tu- and Br-treated cells, while Tg had no negative impact (Fig. 2E). These data corresponded to the level of cell surface FGFR1 expression (Fig. 2B).

ER stress impairs FGFR1, LRP6 and PTH1R maturation in osteogenesis imperfecta (OI)

Next, we turned to OI, a heritable skeletal dysplasia characterized by markedly increased bone fragility along with other systemic involvement [31]. OI is genetically heterogeneous, and the genes involved encode the type I collagen as well as genes involved in ER processing, maturation and secretion of type I procollagen [32]. Extensive ER stress observed in OI osteoblasts is due to ER accumulation of misfolded type I collagen due to missense mutations in *COL1A1* and *COL1A2* genes [33–35]. The *Aga2* is an OI mouse model caused by a heterozygous *Col1a1* mutation with established ER stress [36, 37]. We used *Aga2* mice to determine the effects of ER stress on the biogenesis of transmembrane receptors important for osteoblast function, the low-density lipoprotein receptor-related protein 6 (LRP6), FGFR1, and parathyroid hormone-1 receptor (PTH1R) [38, 39].

Calvarial bones were dissected from wildtype and *Aga2* mice and subjected to FGFR1, LRP6 and PTH1R western blot after removal of suture line tissues (Fig. 3A). FGFR1 migrated as a 130 kDa mature cell surface variant and two immature variants of 108·4 and 91·2 kDa (Fig. 3B) (Table S1). FGFR1 was quantified and expressed relative to actin or GAPDH (Figs. 3C, S11A). We found downregulation of both total FGFR1 (all variants) and cell surface FGFR1 (130 kDa variant) in *Aga2*-derived calvarial osteoblasts. In addition, the proportion of immature 91·2 kDa FGFR1 variant increased (Figs. 3C, S11A), indicating accumulation in the ER. We were unable to distinguish between mature and immature LRP6, due to close migration large 200·9 and 181·7 kDa LRP6 (Fig. 3B). However, similar to FGFR1, expression of total LRP6 was downregulated in *Aga2* osteoblasts compared to control animals (Figs. 3B, D; S11B). In osteoblasts derived from *Aga2* calvaria, PTH1R migrates as a mature 48·6 kDa variant and an immature variant of 45·7 kDa (Fig. 2B). Compared to the wildtype osteoblasts, *Aga2* osteoblasts showed a significant increase in the total amount of (mature and immature) PTH1R, while the proportion of mature (cell surface) PTH1R decreased (Fig. 3E). Our findings show that key receptors involved in osteoblast function, FGFR1, LRP6 and PTH1R, are negatively impacted by ER stress in an OI mouse model.

Next, we investigated how ER stress affected FGFR1 function. Figure 2 shows that ER stress induced by Tu and Br resulted in a decrease in mature FGFR1 in U2OS-FGFR1 cells, with a lesser effect induced by Tg. To determine whether the loss of mature FGFR1 impaired signaling, cells were treated with FGF2 and

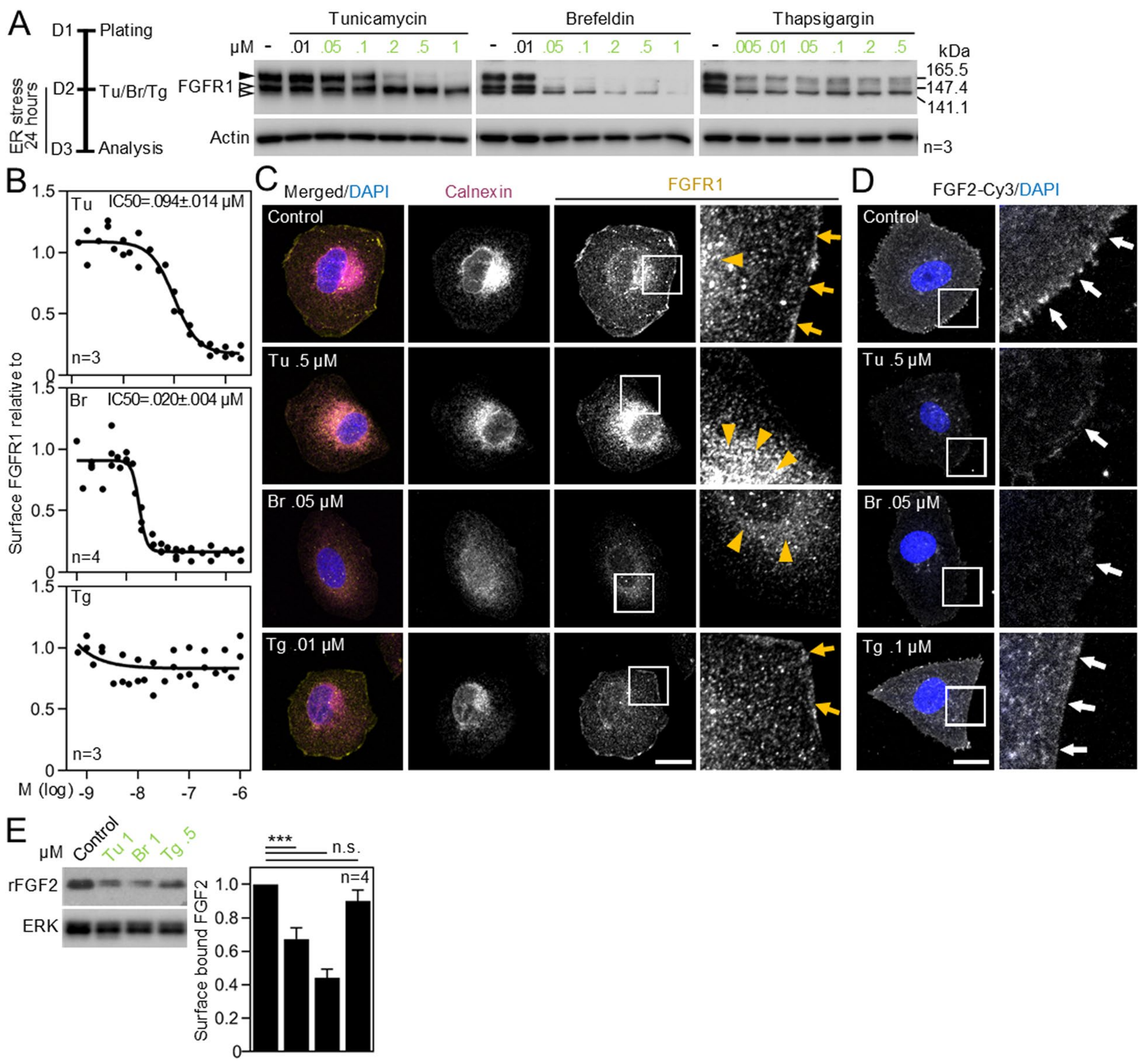

Fig. 2 ER stress and FGFR1 maturation. **A** Short-term ER stress experiments with U2OS-FGFR1 cells. Cells were treated with tunicamycin (Tu), brefeldin (Br) or thapsigargin (Tg) for 24 h (black, no ER stress; green, survivable ER stress; survival data in Fig. S10A-C). FGFR1 expression was analyzed by western blot (black arrowhead, mature FGFR1 at the cell surface; open arrowheads, immature FGFR1). **B** Cell surface FGFR1, determined by flow-cytometry on live cells. IC50 (mean ± S.E.) was calculated for Tu and Br; no changes in surface FGFR1 were found in cells treated with Tg. **C** Subcellular localization of FGFR1; calnexin immunolabeling indicates the ER. Note the absence of cell-surface FGFR1 (arrows) and its accumulation in ER (arrowheads) of cells treated with Tu and Br (scale bar, 10 μm). **D** Cells were treated with Cy3-labelled FGFR1 ligand FGF2, and the cell surface-bound Cy3-FGF2 was visualized by confocal microscopy (arrows). (**E**) Cells were treated with recombinant FGF2 (rFGF2), and the cells surface-associated rFGF2 was determined by western blot. FGF2 signal was normalized to ERK expression, and plotted. Statistical significances were calculated using Student´s *t*-test (*p*<005; ***p*<0·01, ****p*<0·001); n.s. – not significant. Bar plot – mean ± S.E. n, number of independent experiments

analyzed for FGFR1 phosphorylation by western blot. Tu and Br reduced FGF2-mediated phosphorylation of FGFR1 by more than 60%; no effect was observed when treated with Tg (Fig. 3F). This suggests that ER stress causes intracellular retention of FGFR1 which inhibits the ligand-mediated signaling.

Chronic disorders such as OI produce consistently increased levels of ER stress. How does prolonged ER stress affect FGFR1 signaling? To investigate this question, we established a model of prolonged ER stress in which U2OS-FGFR1 cells were treated with Tu for a period of 4–5 days (Fig. 3G). Tu was chosen because it caused only minimal changes of total FGFR1 expression in the 24-h experiments, unlike Br and Tg (Fig. 2A). The cells tolerated the chronic ER stress well, as no effect of Tu on cell proliferation was observed for up to nine days (Fig. S10D-F). FGFR1 flow cytometry on live cells showed that treatment with Tu for 4–5 days reduced cell surface FGFR1 (Fig. 3H) without significantly altering the expression of total FGFR1 protein (Fig. 3I, top blot). This was reflected in signaling, as FGFR1 phosphorylation induced by FGF2 treatment decreased in Tu-treated cells, proportional to the downregulation of mature FGFR1 from the cell membrane (Fig. 3I, middle blot and graph). Our data demonstrate that chronic ER stress leads to impaired cell communication via FGFR1.

LRP6 forms complexes with members of the frizzled family (FZD) at the cell membrane, together serving as receptors for extracellular signals transmitted by morphogens of the WNT family [40, 41]. To further expand on our observation of decreased LRP6 levels in *Aga2* mice (Fig. 3B, D), we treated 293T cells expressing FZD5 or LRP6 with non-toxic Tu, Br and Tg doses. This resulted in partial-to-complete loss of the mature ~ 60 kDa FZD5 and intracellular retention of the immature variants (Fig. 3J) (Table S1). Similar effects of Tu, Br and Tg were observed on maturation of transfected LRP6 in 293T cells (Fig. 3J), and endogenous LRP6 in SAOS2 and RCS cells (Figs. S12, S13A-E). Loss of LRP6 and FZD5 from the cell surface during ER stress can affect the cell response to WNT ligands. We treated SAOS2 cells and RCS with the recombinant WNT ligand WNT3A, and determined LRP6 phosphorylation at serine 1490, which is a hallmark of activation of the WNT pathway [42]. WNT3A-mediated phosphorylation was abrogated by Tu, Br, and Tg (Figs. 3K; S13F-I).

Activation of WNT signaling increases the transcriptional activity of β-catenin. 293T cells stably transfected with the luciferase WNT reporter Super TOPFlash (293T-STF) were used to monitor the induction of transcriptional activity of the WNT/β-catenin pathway [43]. 293T-STF cells were treated with non-toxic doses of Tu, Br and Tg for 24 h, followed by a 24-h treatment with WNT3A. Significant inhibition of WNT3A-mediated TOPFlash transactivation was observed, reaching 89, 59 and 95% reduction in cells treated with Tu, Br and Tg, respectively (Fig. 3L). Our data indicate that maturation of FZD5 and LRP6 is impaired by ER stress and that ER stress inhibits WNT3A-mediated activation of the WNT/β-catenin signaling.

ER stress impairs ROR1 maturation in chronic lymphoid leukemia (CLL)

CLL is caused by a clonal expansion of mature CD5-expressing B cells due to genetic alterations that regulate B cell receptor signaling, DNA damage response, RNA processing, cell cycle, and apoptosis [44]. In CLL cells, the UPR proteins CHOP and BiP were found constitutively upregulated, indicating the presence of ER stress [45]. We collected peripheral blood samples from twelve CLL patients (Fig. 4A) and subjected the isolated B lymphocytes to western blot analysis of ER stress markers. Compared to control B lymphocytes derived from five healthy individuals, CLL cells showed elevated

(See figure on next page.)

Fig. 3 ER stress impairs FGFR1, LRP6 and PTH1R maturation in osteogenesis imperfecta. **A** The postnatal day 4 (P4) mouse skull with indicated calvarias used for sample collection. **B** Calvaria lysates of P4 wildtype (WT) and *Aga2* (OI) mice were immunoblotted for FGFR1, LRP6 and PTH1R; actin and GAPDH served as loading controls. Black arrowhead, mature FGFR1 or PTH1R at the cell surface; open and red arrowheads, immature FGFR1 or PTH1R variants. **C** Total, cell surface (black arrow) and ER (red arrow) FGFR1 signal was quantified by densitometry, normalized to actin or GAPDH (Fig. S11) and presented as values relative to an average WT. **D** Total LRP6 expression was downregulated in *Aga2* mice. **E** Total PTH1R expression was upregulated, and the portion of cell surface (black arrow) PTH1R was downregulated in *Aga2* mice. **F** U2OS-FGFR1 cells were treated with tunicamycin (Tu), brefeldin (Br) or thapsigargin (Tg) for 24 h, stimulated with 100 ng/ml FGF2 for 30 min, and analyzed for FGFR1 phosphorylation (p) by western blot; total FGFR1 levels and actin served as loading controls. pFGFR1 signal was normalized to total FGFR1, and plotted. **G** Chronic ER stress experiments. Cells were treated with Tu for 4–5 days, and analyzed (survival data in Fig. S10D-F). **H** Cell surface FGFR1 expression in cells treated with Tu, determined by flow-cytometry (no Ab, no FGFR1 antibody). **I** Cells were treated with Tu for 4–5 days before treatment with 100 ng/ml FGF2 for 30 min. pFGFR1 signal was normalized to total FGFR1, and plotted. **J** 293T cells were transfected with plasmids expressing FZD5 and LRP6 receptors, and treated with Tu, Br and Tg for 24 h (black, no ER stress; green, non-toxic ER stress; red, toxic ER stress). Cells were analyzed for expression of given proteins by western blot (black arrowhead, mature receptor at the cell surface; open arrowheads, immature receptor isoforms). **K** SAOS2 cells (Fig. S12) were treated with indicated concentrations of Tu, Br and Tg for 24 h, stimulated with WNT3A for 90 min, and immunoblotted for LRP6 phosphorylated (p) at Ser1490. **L** 293T-STF cells were treated with Tu, Br and Tg, and WNT3A. The levels of TOPflash transactivation (fold activation by WNT3A relative to control) were graphed. Statistical significances were calculated using Student´s *t*-test ($p < 0.05$; ** $p < 0.01$, *** $p < 0.001$); n.s. – not significant. Bar plots – mean ± S.E. Scatter plots – individual animals (open circles) and mean ± S.E. n, number of independent experiments

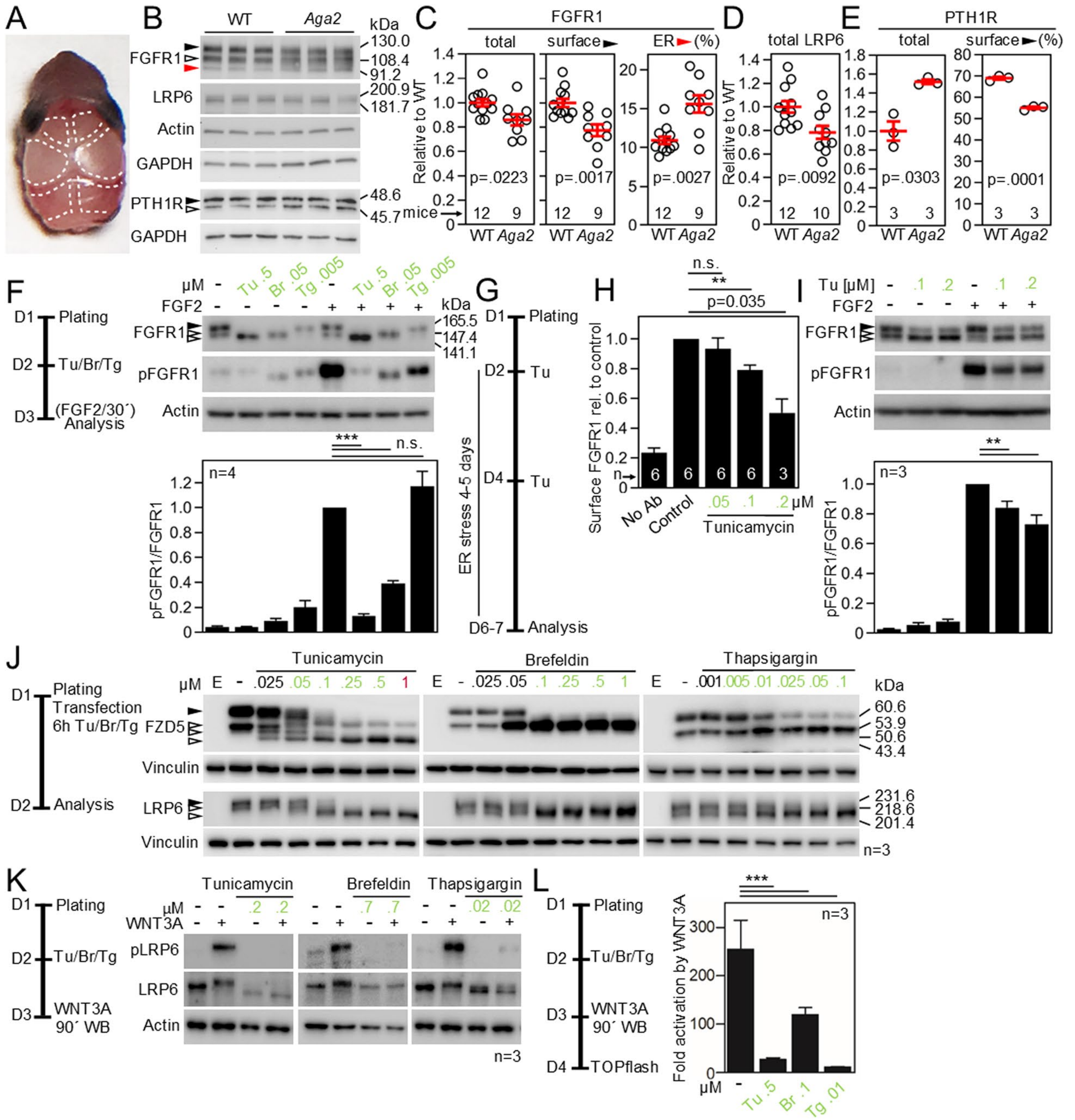

Fig. 3 (See legend on previous page.)

levels of ATF4, ATF6, HERPUD1, IRE1a, XBP1s, BiP and CHOP (Fig. 4B, C). Next, we investigated whether the biogenesis of transmembrane receptors is impaired in CLL. The receptor tyrosine kinase-like orphan receptor (ROR1) was selected because it is highly expressed by CLL cells and represents an important oncogene and therapy target [46, 47]. ROR1 was expressed in all CLL samples and migrated on the acrylamide gel as a mature variant of 122·9 kDa and two immature variants (112·7 and 108·3 kDa) (Fig. 4B) (Table S1). This corresponded to the three variants of ROR1 (125·3, 199·3, 112·3 kDa) detected in Tu-, Br- or Tg-treated 293T cells expressing transgenic ROR1 (Fig. 4D). The extent of ER retention of ROR1 in CLL cells, including increased expression of the immature forms, correlated positively with the ER stress marker expression, peripheral blood leukocyte concentration, the absence of IGHV hypermutation (which is associated with increased disease progression), and the presence of TP53 mutations (Fig. 4E-G). Increased ER retention of ROR1 was also observed in patients who had previously undergone therapy.

BiP expression or treatment with TUDCA restore receptor maturation and signaling during ER stress

Next, we addressed the question of whether the disrupted receptor signaling during ER stress can be restored. Treatment of RCS cells with FGF2 resulted in activation of the ERK pathway; this activation was inhibited by treatment with a non-toxic concentration of Tu (Fig. 5A). Similarly, the FGF2-mediated phosphorylation of signaling adapters FRS2 and GAB1, which regulate the relay of signal from FGFRs to ERK pathway [48] was inhibited by ER-stress (Fig. S14). The pKrox24(MapERK)Luc reporter, which expresses firefly luciferase [49], was used to monitor the transcriptional activity of the FGF2-mediated ERK pathway. In RCS cells stably expressing the pKrox24 (Table S2), treatment with FGF2 resulted in an approximately 26-fold increase in pKrox24 transactivation compared to untreated controls (Fig. 5B); this transactivation was significantly reduced by Tu. The negative effect of Tu on FGF2 signaling was partially restored when cells were treated with the recently developed recombinant FGF2-STAB protein, which exhibits increased thermal stability and biological activity [50] (Fig. 5C). Thus, treatment with more potent ligand can partially compensate for the reduction of cell surface receptors due to ER stress.

Treatment of 293T cells with Tu resulted in a strong induction of BiP (Fig. S5B), which functions as an ER-resident chaperone that is upregulated during the UPR [51] (Fig. S1). Expression of BiP together with FGFR3 in 293T cells rescued the Tu effect on FGFR3 biogenesis, as evidenced by a reduction in ER retention of immature FGFR3 and a corresponding upregulation of FGFR3 at the cell surface (Fig. 5D); similar data were obtained in 293T-FGFR3 cells (Fig. S15A). This suggests that supporting the adaptive UPR by elevating the cellular levels of BiP stabilizes cell surface FGFR levels.

Restoration of ER function by pharmacological chaperones can reverse impaired receptor biogenesis and signaling. We developed a cellular assay to screen for molecules that restore receptor signaling disrupted by ER stress. This consisted of a pKrox24 transcriptional reporter linked to DsRed [49], inserted in RCS cells stably expressing a weakly activating FGFR3 variant (FGFR3-G380R) (Table S2). Treatment of RCS-FGFR3-G380R:pKrox24-DsRed cells with FGF2 resulted in DsRed accumulation as determined by western blot or fluorescence imaging (Fig. 5E, F). Tu downregulated mature FGFR3-G380R and inhibited the induction of DsRed by FGF2, monitored by automated microscopy for 24 h. Both cellular phenotypes were restored by treatment with tauroursodeoxycholic acid (TUDCA) (Figs. 5G-I; S15B). TUDCA has several proposed mechanisms to reduce ER stress, including inhibition of dissociation between BiP and PERK, resulting in reduced ER stress-mediated cell death and stabilization of the UPR [52]. In U2OS-FGFR1 cells, TUDCA restored Tu-mediated loss of FGFR1 cell surface expression, as shown by western blot for FGFR1 isoform expression (Fig. S15C) and FGFR1 flow cytometry on live cells (Fig. 5J, K). The FGFR1 signaling was also restored by TUDCA, as shown by the analysis of FGF2-mediated FGFR1 phosphorylation (Fig. 5L). These data suggest that ER stress alleviation by TUDCA restores transmembrane receptor maturation and signaling.

Discussion

In summary, we show that loss of transmembrane receptor signaling is associated with ER stress and thus impairs the cell's ability to communicate, further contributing to the pathologies caused by or accompanied by ER stress. Our results show that ER stress leads to

(See figure on next page.)

Fig. 4 ER stress impairs ROR1 maturation in chronic lymphoid leukemia. **A** CLL patient status at the time when the peripheral blood biopsy was taken. Leu, the number of leukocytes per liter. FCR, Fludarabine, cyclophosphamide and rituximab; M, mutated IGHV. Minor M/mM, mutation detected in *TP53* present with less than 5% variant allele frequency; CK, complex karyotype; Neg., negative. **B** B cells purified from CLL patients and healthy controls were analyzed by western blot for the expression and migration pattern of ROR1 and for the UPR markers PERK, ATF4, ATF6, HERPUD1, IRE1α, XBP1s, BiP and CHOP; actin was used as a loading control. Note the various degree of ER accumulation of ROR1 (black arrowhead, mature receptor at the cell surface; open arrowheads, immature receptor in the ER), and of ER stress among the CLL patients. **C** The UPR marker expression was analyzed by densitometry, normalized to actin and plotted as a ratio to an average healthy control (red dashed line). **D** 293T cells were transfected with C-terminally V5-tagged human ROR1 and treated with tunicamycin, brefeldin and thapsigargin for 24 h (black, no ER stress; green, non-toxic ER stress; red, toxic ER stress). Cells were analyzed for ROR1 expression by western blot (black arrowhead, mature ROR1 at the cell surface; open arrowheads, immature ROR1). **E** The ER ROR1 levels correlate with ER stress levels in CLL. The percentage of ER ROR1 in the 12 analyzed CLL patients was plotted against UPR expression levels. **F** The ER ROR1 levels correlate with leukocyte counts in the peripheral blood of individuals with CLL. **G** The ER ROR1 levels correlate with the IGHV and *TP53* mutation status, and the prior therapy. Statistical significances were calculated using Student´s *t*-test ($p < 0·05$; ** $p < 0·01$, *** $p < 0·001$); n.s. – not significant. Bar plots – mean ± S.E. Box and whiskers – min–max 10–90%. Scatter plots – individual patients (open triangles) and linear regression (red line and the r^2 and p values). n, number of individuals or independent experiments

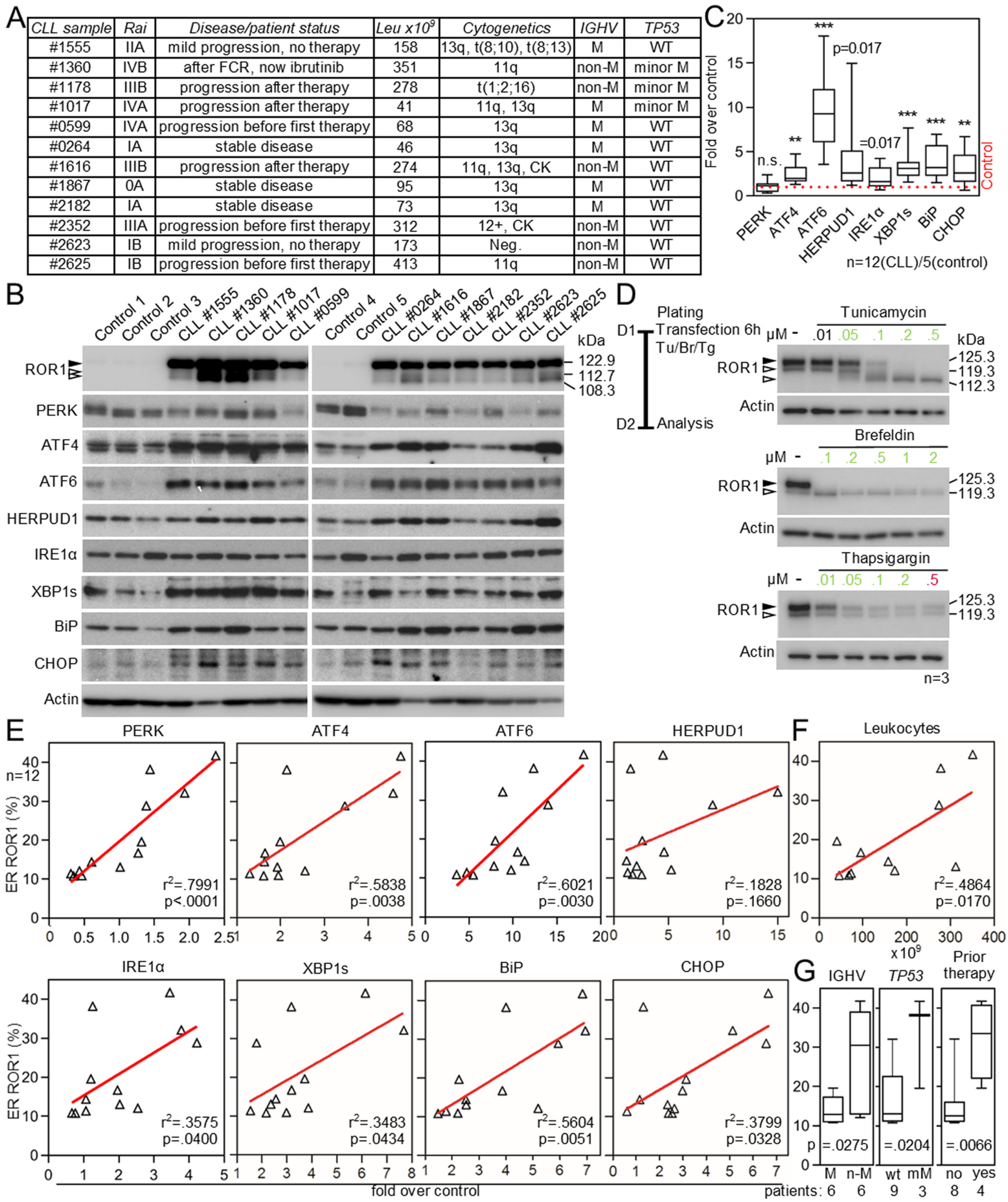

Fig. 4 (See legend on previous page.)

decreased expression of ER trafficked receptors, which is due to downregulated receptor synthesis and intracellular receptor retention (Fig. 6). These findings were not limited to a single receptor, but affected the receptor tyrosine

kinases FGFR1 and FGFR3, the pseudokinase receptor ROR1, the WNT signaling pathway receptors LRP6 and FZD5, and the parathyroid hormone receptor PTH1R, suggesting that ER stress affects a variety of cell communication systems. Why transmembrane receptors are sensitive to ER stress may be due to their tight regulation, which prevents uncontrolled activation that underlies many abnormal proliferative states. Once activated, transmembrane receptors are rapidly internalized. For FGFR1, treatment of cells with FGF triggers immediate internalization, as most FGF-FGFR1 complexes are localized to early endosomes 5–15 min after stimulation [53–55]. The endocytosed FGFR1 is degraded by the lysosome to suppress signaling, so that two hours after stimulation by the ligand, hardly any FGFR1 can be detected in the cells [54]. This rapid turnover requires a constant production of new receptor molecules. Since the newly produced receptors constantly traverse the ER-Golgi system, their biogenesis is particularly susceptible to ER deterioration compared to other proteins with slower turnover, such as components of the ECM. In addition, receptors are physiologically expressed at low levels, providing a strong barrier against uncontrolled signaling, but also placing increased demands on production. Finally, many receptors are unstable proteins that are highly dependent on chaperones to support their folding and stability [56–58]. Our demonstration that ER stress affects membrane receptor availability has broad physiological significance, as demonstrated for multiple myeloma (MM) and FGFR3 and in osteogenesis imperfecta (OI) for FGFR1 and LRP6.

In MM, ER stress led to downregulation of receptors at the cell membrane and impaired signaling, as demonstrated for FGFR3. Induction of ER stress may be an effective strategy to reduce the expression of oncogenic receptors, as we have shown with bortezomib (Bz). The results suggest an alternative mechanism of action of bortezomib in MM: induction of ER stress leading to a reduction in FGFR3 and ERK signaling at the membrane, a known driver of MM pathology. As in MM, induction of ER stress may be beneficial in certain cancers, and treatments that take advantage of this cellular response could be concerned. Conversely, high ER stress is associated with many cancers, including blood malignancies [2]. Perhaps not surprisingly, high levels of UPR signaling can correlate with poor prognosis [59–64], probably because previously presented antigens are hidden within cells and often misfolded, making it difficult for immune cells, monoclonal antibodies, or kinase inhibitors to intervene. This suggests that UPR signaling is not only tolerated but even favored by some cancers. Here we show that increased ER stress in CLL negatively correlates with ROR1 membrane expression (Fig. 4). The presence of fully matured ROR1 positively correlated with expression of downstream mediators of ROR1 signaling Vangl2 and Dvl2 [65] in CLL cells, suggesting that different levels of ER stress may regulate ROR1 signaling and oncogenic potential. A ROR1 immunotherapy is in development [47], but our data suggest that the sensitivity of ROR1 to ER stress and its membrane expression may influence response. We also found that conventional CLL therapy likely increases ER stress, which may contribute to disease progression by reducing the availability of therapeutic targets. This suggests that ER stress therapy could restore cell membrane presentation of antigenic targets and improve CLL disease outcome.

(See figure on next page.)

Fig. 5 BiP and TUDCA restore cell surface receptor levels and signaling during ER stress. **A** Phosphorylation (p) of ERK MAP kinase in RCS cells treated by FGFR3 ligand FGF2. Vinculin and total ERK serve as loading controls. Relative pERK levels were determined and plotted on the right. **B** FGF2-mediated activation of FGFR3 signaling RCS cells, determined by transactivation of pKrox24 transcriptional reporter coupled with firefly luciferase; data were expressed as fold induction relative to untreated control. **C** Inhibition of FGF2-mediated pKrox24 transactivation by Tu was partially rescued by treatment with the thermally stable (S) variant of FGF2. **D** 293T cells were co-transfected with FGFR3 and BiP-Flag, treated with tunicamycin (Tu), and analyzed by western blot 24 h later. Percentage of ER (red arrowhead) and surface (black arrowhead) FGFR3 was obtained by densitometry and plotted. **E**, **F** RCS-FGFR3-G380R::pKrox24-DsRed cells were treated with FGF2, and the DsRed induction was monitored by western blot (E) or live cell imaging (F; scale bar 50 µm). **G** Cells were treated with Tu and TUDCA, and analyzed by western blot 48 h later (H), or treated with FGF2 and monitored by automated microscopy for additional 24 h (I). **H** TUDCA restored Tu-induced loss of surface FGFR3 (black arrowhead, mature FGFR3 at the cell surface; open arrowheads, immature FGFR3 variants). HERPUD1 was used to monitor ER stress, vinculin served as loading control (signal quantifications at Fig. S15B). **I** TUDCA restored Tu-induced loss of FGF2-mediated pKrox24-DsRed transactivation, monitored by live cell imaging. **J** U2OS-FGFR1 cells were treated with Tu and TUDCA for 48 h, and the surface levels of FGFR1 and its signaling were monitored by flow-cytometry (K) and western blot (L). **K** TUDCA restored Tu-mediated loss of surface FGFR1. Note the increase of surface FGFR1 produced by TUDCA alone. **L** TUDCA restored Tu-induced loss of FGF2-mediated FGFR1 phosphorylation (p) (graph, signal quantification). BiP was used to monitor ER stress, actin serves as loading control. Statistical significances were calculated using Student´s *t*-test ($p <$ 0·05; ** $p <$ 0·01, *** $p <$ 0·001); n.s. – not significant. Bar and line plots – mean ± S.E. n, number of independent experiments

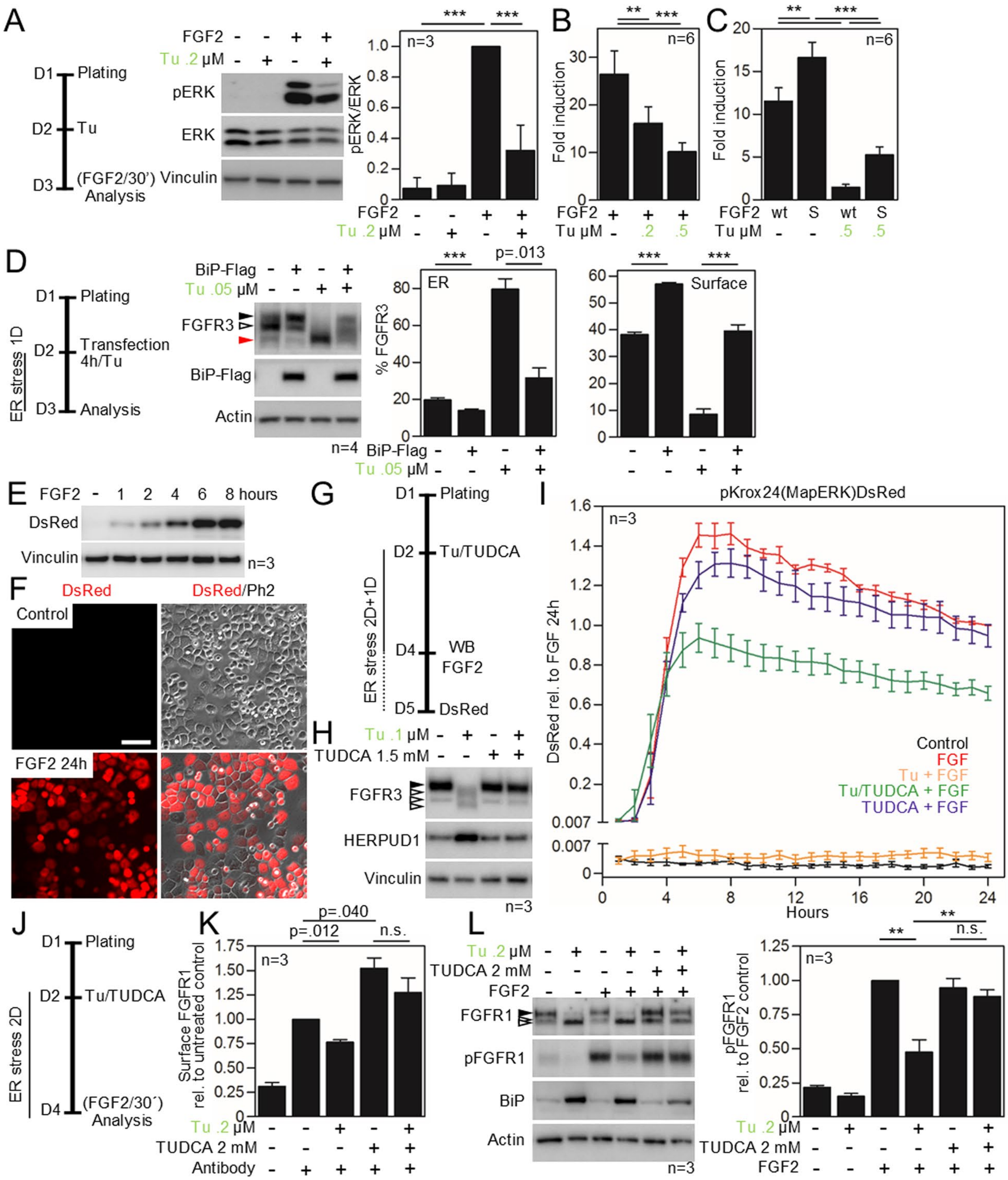

Fig. 5 (See legend on previous page.)

Even mild, non-toxic ER stress, which did not affect cell proliferation, resulted in a significant downregulation of cell surface receptors, as shown in U2OS-FGFR1 cells exposed to short-term or prolonged ER stress (Fig. 3F-I). The resulting changes in the cell's response to its extracellular environment are likely to alter cell function and need to be considered in studies addressing the mechanisms of cell communication in both physiological and

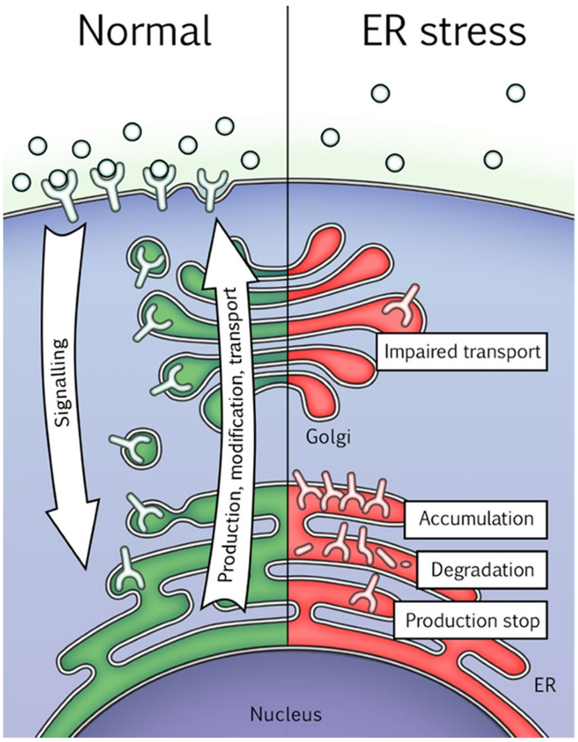

Fig. 6 ER stress disrupts signaling via altered processing of transmembrane receptors. Transmembrane receptors transition through the ER-Golgi system during their biogenesis. When folded, modified and matured, the receptors are presented at the cell surface, bind their cognate ligands and initiate downstream signaling. Deterioration of ER function during ER stress alters receptor production, causes improper folding and degradation, or interferes with transport causing intracellular receptor accumulation. Collectively, these changes lead to loss of signaling-competent receptor molecules at the cell surface and impaired communication

pathological situations. One of the strengths of this study is that the insights gained in vitro on the effects of ER stress on receptor maturation and cell surface receptor content could also be observed in vivo, as exemplified in OI.

Reduced levels of mature membrane receptors were detected in the calvarial bone of the Aga2 mouse, an established model for OI (Fig. 3A-E). Endogenous ER stress induced the downregulation of mature FGFR1 and increased the concentration of immature intracellular FGFR1. Conditional loss of FGFR1 in osteoprogenitors increases proliferation and delays differentiation and matrix mineralization, whereas loss of FGFR1 in committed osteoblasts promotes cortical mineralization and thickening [39, 66]. Interestingly, low bone mass and high fragility is a hallmark of OI, while a specific feature of OI is that the bone matrix is abnormally highly mineralized [67, 68]. The etiology of this paradox is not known, but our results suggest that loss of FGFR1 signaling due to ER stress in osteoblasts through the effects on osteoprogenitors and then mature osteoblasts may be a factor leading to delayed osteoblast differentiation and then increased mineralization.

In vitro modeling of ER stress in several cell lines, including 293T, RCS and SAOS2, also negatively affected the expression levels of the mature WNT receptors FZD5 and LRP6 (Figs. 3J-L, S13). WNT signaling is an important regulatory pathway in osteogenic differentiation that promotes bone formation [69], and loss of WNT signaling due to mutations in WNT1 or LRP5 leads to undermineralized bone disorders, an autosomal recessive form of OI, and osteoporosis-pseudoglioma syndrome, respectively. In each of these disorders, loss of proper WNT signaling contributes to the disease phenotype [70, 71]. Mouse models of OI showed impaired differentiation of osteoblasts and mesenchymal stem cells, respectively [72, 73]. Similar to altered FGF signaling, loss of signaling due to ER stress and decreased availability of the mature WNT signaling receptor negatively affects osteoblasts and may contribute to osteoblastic dysfunction in OI. Finally, endogenous ER stress in Aga2 osteoblasts increased the total amount of PTH1R protein and also immature PTH1R. The role of PTH signaling mediated by PTH1R is complex. Abnormal constitutive PTH/PTH1R activity increases bone resorption, but intermittent activity has a positive anabolic effect on osteoblasts. These effects include increased proliferation and differentiation of osteoblasts, reduction of osteoblast apoptosis, and enhancement of the WNT/b-catenin signaling pathway [74]. Dysregulation of PTH1R expression is likely a further contributor to low bone mineral density and propensity to fracture in OI.

Our research demonstrates the collateral damage of ER stress on cellular communication and emphasizes the reversibility of the negative impact of ER stress on transmembrane receptor levels. We found that impaired receptor signaling can be restored by cell treatment with designer ligands, such as stabilized FGF2, or pharmacological chaperones that reverse ER stress and restore receptor biogenesis (Fig. 5). These findings could be exploited in disease treatment strategies by either alleviating or inducing ER stress to effectively modulate cellular signaling. Finally, while precision medicine often addresses the importance of underlying genetic variation in disease, our findings suggest that while germline and somatic mutation are important targets, appreciating their effect on cellular biology, particularly ER stress, needs to be considered for as targeted treatments are employed.

Methods

Cell culture, vectors, transfection and luciferase reporter assay

Table S2 lists the cell lines used in the manuscript. Cells were propagated in DMEM (293T, RCS, U2OS), RPMI1640 (KMS11, KMS18) or McCoy's 5a (SAOS2), supplemented with 10% or 15% (SAOS2) FBS and antibiotics (Invitrogen). RCS-FGFR3-G380R:pKrox24-DsRed cells were derived from RCS-FGFR3-G380R cells [75] using piggyBac transposase for stable integration of the TR01F plasmid [76] where the GFP encoding sequence was removed and NF-κB responsive element with Luc2 gene were replaced by pKrox24(MapErk)DsRed reporter [49]. 293T-FGFR3 cells were derived from 293T using piggyBac transposase which stably integrated TR01F plasmid containing truncated CMV promotor and hFGFR3-V5 coding sequence. Recombinant FGF2 and WNT3A were obtained from RnD Systems; recombinant FGF2-STAB was from Enantis; recombinant FGF2-Cy3 was a kind gift from Prof. Lars Klimaschewski (Medizinische Universität Innsbruck, Austria). TUDCA and KIRA6 were from Sigma; tunicamycin, brefeldin A, thapsigargin, bortezomib, sephin 1, PF429242, AA147 and APY-29 were from Tocris; GSK2606414 was from Merck. Cells were transfected using the FuGENE6 reagent (Promega), Lipofectamine 2000 (Invitrogen), or by electroporation using the Neon Transfection System (Invitrogen). Table S3 lists all vectors used for transfection. For the luciferase assay, the pKrox24(MapERK)Luc firefly luciferase reporter [49] was transfected together with the pTK-RL vector (Promega) in 3:1 (μg of DNA) ratio into RCS cells, as previously described [77]. Cells were stimulated with 5 ng/ml of recombinant FGF2 or FGF2-STAB for 24 h, and the luciferase signal was determined using dual-luciferase assay (Promega). 293T-STF cells were analyzed for luciferase activity similar to RCS cells.

Western blot, deglycosylation assay and FGF2-binding assay

For western blot, cells were harvested directly into the 2xLaemmli sample buffer. Cell lysates were resolved by SDS-PAGE, transferred onto a PVDF membrane and visualized by chemiluminescence (Thermo). Table S4 lists the antibodies used for western blots. The pictures were taken on a Fusion Solo device (Vilber). Digitally acquired overlays of protein ladder migration and luminescent signal from at least two exposures of three independent experiments were used to determine the molecular mass of analyzed receptors (Table S1), which was calculated from polynomic regression equation fitted on the migration of 10–250 kDa PageRuler Plus Ladder (Thermo). Figure S16 shows the position of closest ladder protein for each of the analyzed non-receptor proteins when it first appeared in the manuscript. Western blot signal was quantified in ImageJ. For the FGFR3 deglycosylation assay, transfected 293T cells were lysed in RIPA buffer (50 mM tris–HCl pH 7·4, 150 mM NaCl, 0·5% NP- 40, 0·25% sodium deoxycholate, 2 mM EDTA, 1 mM Na_3VO_4 and protease inhibitors (Roche) at 4 °C/30 min, and cleared by 13,000 g/4 °C/15 min. Supernatants were mixed with 0·5U of PNGase F (Roche), incubated at 37 °C/6 h and mixed with 5xLaemmli. For FGF2 binding, the U2OS cells were incubated with ice cold 2%BSA/PBS containing 100 ng/ml FGF2 on ice for 30´, incubated at 37 °C for 30´, washed twice and lysed. Boiled cell lysates were resolved by SDS-PAGE, transferred onto a PVDF membrane and visualized by chemiluminescence (Thermo).

Immunocytochemistry, live-cell imaging and flow-cytometry

For immunocytochemistry, cells were fixed in paraformaldehyde and permeabilization by 0·1% Triton-X100/PBS was used. Images were taken on a Carl Zeiss LSM700 laser scanning microscope with acquisition using the ZEN Black 2012 software. DsRed fluorescence was determined by automated microscopy (Nikon BioStation). Phase contrast and fluorescence signal images were automatically acquired every hour during a 24 h period. Signal was normalized to cell amounts in each image acquired from phase contrast. For flow cytometry, pelleted cells were incubated with the antibodies diluted in wash buffer (10%FBS/PBS) on ice/30 min, washed and the fluorescence was detected using BD FACS Aria II; the analysis was done in FlowJo (BD Life Sciences). Table S4 lists antibodies used for immunocytochemistry and flow cytometry.

Human B lymphocytes

Peripheral blood samples were obtained from CLL patients during routine testing at the University Hospital Brno Czech Republic. CLL cells were separated using immunodensity negative selection (RosetteSep™ Human B Cell Enrichment Cocktail, RosetteSep™ Human CD3 Depletion Cocktail; STEMCELLS Technologies). The purity was 95–99%, as determined by flow-cytometry. Similarly, the B-lymphocytes were separated from buffy coats obtained from healthy volunteers, with 80–92% purity. For all samples, written informed consent approved by the Ethical Committee of University Hospital Brno was given in accordance with the Declaration of Helsinki. For western blot analysis, the cells were lysed in RIPA buffer, cleared by centrifugation, and mixed with 5xLaemmli sample buffer.

Animal experiments
Aga2$^{+/-}$ animals were maintained in a C57BL/6 background [36]. The*Aga2*$^{+/-}$ colony was maintained through mutant alleles only passed through males. Both male and female animals were studied. All animal studies were terminated at P4 and euthanasia was performed via isoflourane inhalation and cervical dislocation according to AALAC protocols. Calvarial lysates were extracted from dissected P4 calvaria with suture line tissues removed and flash frozen in liquid nitrogen. Cells were extracted from frozen calvarial tissues via mortal and pestle and lysed in RIPA buffer (Millipore) supplemented with Halt Protease and Phosphatase Inhibitor (Thermo). The concentrations of a total 22 (12 wildtype and 10 Aga2) calvaria lysates were determined using the Pierce BCA Protein Assay Kit (Thermo). Samples were subjected to SDS-PAGE electrophoresis on 4–20% gradient gels (BioRad). Chemiluminescent and colorimetric images were taken on a ChemiDoc Touch Imaging System (BioRad).

Statistical analyses and adjustment of microphotographs
All experiments were performed at least in triplicates unless stated otherwise. The *n* values express the actual number of independent biological experiments, and are stated in each figure panel. In the bar and line graphs, data are presented as mean ± S.E. The scatter plots show individual animals or patients. The min-max in the box and whisker plots are defined by 10th-90th percentiles. Two-tailed Student´s *t*-test was used for statistical evaluation of differences. Brightness and contrast were adjusted in microphotographs, homogenously throughout each panel.

Data sharing
All data generated or analyzed in the study are available from the corresponding authors on reasonable request.

Supplementary Information
The online version contains supplementary material available at https://doi.org/10.1186/s12964-025-02208-w.

Additional file 1.

Acknowledgements
We thank to Lars Klimaschewski for FGF2-Cy3, Petr Mores for help with the figure animation and Marie Tesarova for excellent technical assistance.

Authors' contributions
MB, SPA, AAC, AK, V-CU, ZF, GR-L, AN, KSv, PKo, BF, TG, PKr conducted cell experiments; JK, MD, JM, MB, SPA, AN collected and analyzed patient samples; DW, JTZ, AK, ID conducted animal experiments; MB, PV, DK, KSo, PKr designed research and analyzed data; MB, DK, PKr wrote the manuscript, with contribution of all other authors; KSo, DK and PKr provided funds.

Funding
This work was supported by National Institute for Cancer Research (Programme EXCELES, ID Project No. LX22NPO5102) - Funded by the European Union - Next Generation EU; Ministry of Education, Youth and Sports of the Czech Republic (LUAUS23295); Agency for Healthcare Research of the Czech Republic (NU23-10-00550); Czech Science Foundation (GA21-11585S, GF21-26400K). PKr was supported Praemium Academiae of the Czech Academy of Sciences. JK, MD, JM were supported by MH CZ - DRO (FNBr, 65269705). DK was supported by NIH AR 006124 and NIH P01 HD070394. JTZ was supported by a Geisman award from the Osteogenesis Imperfecta Foundation. AN and SPA were supported by IGA MUNI (CZ.02.2.69/0.0/0.0/19_073/0016943). AN was supported by Brno Ph.D. Talent Scholarship - Funded by the Brno City Municipality.

Data availability
All data generated or analyzed in the study are available from the corresponding authors on reasonable request.

Declarations

Competing interests
The authors declare no competing interests.

Received: 28 November 2024 Accepted: 17 April 2025
Published: 30 April 2025

References

1. Hetz C, Zhang K, Kaufman RJ. Mechanisms, regulation and functions of the unfolded protein response. Nat Rev Mol Cell Biol. 2020;21(8):421–38.
2. Wang M, Kaufman RJ. The impact of the endoplasmic reticulum protein-folding environment on cancer development. Nat Rev Cancer. 2014;14(9):581–97.
3. Cox JS, Shamu CE, Walter P. Transcriptional induction of genes encoding endoplasmic reticulum resident proteins requires a transmembrane protein kinase. Cell. 1993;73:1197–206.
4. Harding HP, Zhang Y, Ron D. Protein translation and folding are coupled by an endoplasmic-reticulum-resident kinase. Nature. 1999;397:271–4.
5. Haze K, Yoshida H, Yanagi H, Yura T, Mori K. Mammalian transcription factor ATF6 is synthesized as a transmembrane protein and activated by proteolysis in response to endoplasmic reticulum stress. Mol Biol Cell. 1999;10:3787–99.
6. Frantz C, Stewart KM, Weaver VM. The extracellular matrix at a glance. J Cell Sci. 2010;123(24):4195–200.
7. Moscatelli D. High and low affinity binding sites for basic fibroblast growth factor on cultured cells: absence of a role for low affinity binding in the stimulation of plasminogen activator production by bovine capillary endothelial cells. J Cell Physiol. 1987;131:123–30.
8. Liuzzo J, Moscatelli D. Human Leukemia Cell Lines Bind Basic Fibroblast Growth Factor (FGF) on FGF Receptors and Heparan Sulfates: Downmodulation of FGF Receptors by Phorbol Ester. Blood. 1996;87:245–55.
9. Blair HC, Larrouture QC, Li Y, Lin H, Beer-Stoltz D, Liu L, et al. Osteoblast Differentiation and Bone Matrix Formation In Vivo and In Vitro. Tissue Eng Part B Rev. 2017;23:268–80.
10. Li Y, Kang K, Krahn JM, Croutwater N, Lee K, Umbach DM, et al. A comprehensive genomic pan-cancer classification using The Cancer Genome Atlas gene expression data. BMC Genomics. 2017;3;18(1):508
11. Dai C, Dai S, Cao J. Proteotoxic stress of cancer: implication of the heat-shock response in oncogenesis. J Cell Physiol. 2012;227:2982–7.
12. Shi H, O'Reilly VC, Moreau JLM, Bewes TR, Yam MX, Chapman BE, et al. Gestational stress induces the unfolded protein response, resulting in heart defects. Development (Cambridge). 2016;143:2561–72.
13. Thangaraj A, Sil S, Tripathi A, Chivero ET, Periyasamy P, Buch S. Targeting endoplasmic reticulum stress and autophagy as therapeutic approaches for neurological diseases. Int Rev Cell Mol Biol. 2020;350:285–325.

14. Sprenkle NT, Sims SG, Sánchez CL, Meares GP. Endoplasmic reticulum stress and inflammation in the central nervous system. Mol Neurodegener. 2017;12(1):42.
15. Yadav RK, Chae S-W, Kim H-R, Chae HJ. Endoplasmic Reticulum Stress and Cancer. J Cancer Prev. 2014;19:75–88.
16. Back SH, Kaufman RJ. Endoplasmic reticulum stress and type 2 diabetes. Annu Rev Biochem. 2012;81:767–93.
17. Todd DJ, Lee AH, Glimcher LH. The endoplasmic reticulum stress response in immunity and autoimmunity. Nat Rev Immunol. 2008;8(9):663–74.
18. Kazandjian D. Multiple myeloma epidemiology and survival: A unique malignancy. Semin Oncol. 2016;43:676–81.
19. Nikesitch N, Lee JM, Ling S, Roberts TL. Endoplasmic reticulum stress in the development of multiple myeloma and drug resistance. Clin Transl Immunology. 2018;7(1):e1007. https://doi.org/10.1002/cti2.1007.
20. Obeng EA, Carlson LM, Gutman DM, Harrington WJ, Lee KP, Boise LH. Proteasome inhibitors induce a terminal unfolded protein response in multiple myeloma cells. Blood. 2006;107:4907–16.
21. Curran MP, McKeage K. Bortezomib: A review of its use in patients with multiple myeloma. Drugs. 2009;69:859–88.
22. Chesi M, Nardini E, Brents LA, Schröck E, Ried T, Kuehl WM, et al. Frequent translocation t(4;14)(p16.3;q32.3) in multiple myeloma is associated with increased expression and activating mutations of fibroblast growth factor receptor 3. Nat Genet. 1997;16:260–4
23. Krejci P, Krakow D, Mekikian PB, Wilcox WR. Fibroblast Growth Factors 1, 2, 17, and 19 Are the Predominant FGF Ligands Expressed in Human Fetal Growth Plate Cartilage. Pediatr Res. 2007;61:267–72.
24. Heifetz A, Keenan RW, Elbein AD. Mechanism of action of tunicamycin on the UDP-GlcNAc:dolichyl-phosphate Glc-NAc-1-phosphate transferase. Biochemistry. 1979;18:2186–92.
25. Helms JB, Rothman JE. Inhibition by brefeldin a of a Golgi membrane enzyme that catalyses exchange of guanine nucleotide bound to ARF. Nature. 1992;360:352–4.
26. Sehgal P, Szalai P, Olesen C, Praetorius HA, Nissen P, Christensen SB, et al. Inhibition of the sarco/endoplasmic reticulum (ER) Ca2+-ATPase by thapsigargin analogs induces cell death via ER Ca2+ depletion and the unfolded protein response. J Biol Chem. 2017;292:19656–73.
27. Schröder M, Kaufman RJ. ER stress and the unfolded protein response. Mutation Research - Fundamental and Molecular Mechanisms of Mutagenesis. Mutat Res; 2005;569(1–2):29–63
28. Wang L, Perera BGK, Hari SB, Bhhatarai B, Backes BJ, Seeliger MA, et al. Divergent allosteric control of the IRE1α endoribonuclease using kinase inhibitors. Nat Chem Biol. 2012;8:982–9.
29. Ghosh R, Wang L, Wang ES, Perera BGK, Igbaria A, Morita S, et al. Allosteric inhibition of the IRE1α RNase preserves cell viability and function during endoplasmic reticulum stress. Cell. 2014;158:534–48.
30. Kostas M, Haugsten EM, Zhen Y, Sørensen V, Szybowska P, Fiorito E, et al. Protein Tyrosine Phosphatase Receptor Type G (PTPRG) Controls Fibroblast Growth Factor Receptor (FGFR) 1 Activity and Influences Sensitivity to FGFR Kinase Inhibitors. Mol Cell Proteomics. 2018;17:850–70.
31. Marini JC, Forlino A, Bächinger HP, Bishop NJ, Byers PH, De Paepe A, et al. Osteogenesis imperfecta. Nat Rev Dis Primers. 2017;3:17052. https://doi.org/10.1038/nrdp.2017.52.
32. Claeys L, Storoni S, Eekhoff M, Elting M, Wisse L, Pals G, et al. Collagen transport and related pathways in Osteogenesis Imperfecta. Hum Genet. 2021;140:1121–41.
33. Duran I, Nevarez L, Sarukhanov A, Wu S, Lee K, Krejci P, et al. HSP47 and FKBP65 cooperate in the synthesis of type I procollagen. Hum Mol Genet. 2014;24:1918–28.
34. Mirigian LS, Makareeva E, Mertz EL, Omari S, Roberts-Pilgrim AM, Oestreich AK, et al. Osteoblast Malfunction Caused by Cell Stress Response to Procollagen Misfolding in α2(I)-G610C Mouse Model of Osteogenesis Imperfecta. J Bone Miner Res. 2016;31:1608–16.
35. Lietman CD, Rajagopal A, Homan EP, Munivez E, Jiang MM, Bertin TK, et al. Connective tissue alterations in Fkbp10-/- mice. Hum Mol Genet. 2014;23:4822–31.
36. Lisse TS, Thiele F, Fuchs H, Hans W, Przemeck GKH, Abe K, et al. ER stress-mediated apoptosis in a new mouse model of Osteogenesis imperfecta. PLoS Genet. 2008;4(2):e7. https://doi.org/10.1371/journal.pgen.0040007.
37. Duran I, Zieba J, Csukasi F, Martin JH, Wachtell D, Barad M, et al. 4-PBA Treatment Improves Bone Phenotypes in the Aga2 Mouse Model of Osteogenesis Imperfecta. J Bone Miner Res. 2022;37(4):675–86.
38. Joeng KS, Schumacher CA, Zylstra-Diegel CR, Long F, Williams BO. Lrp5 and Lrp6 redundantly control skeletal development in the mouse embryo. Dev Biol. 2011;359:222–9.
39. Jacob AL, Smith C, Partanen J, Ornitz DM. Fibroblast growth factor receptor 1 signaling in the osteo-chondrogenic cell lineage regulates sequential steps of osteoblast maturation. Dev Biol. 2006;296:315–28.
40. Pinson KI, Brennan J, Monkley S, Avery BJ, Skarnes WC. An LDL-receptor-related protein mediates Wnt signalling in mice. Nature. 2000;407:535–8.
41. Ishikawa TO, Tamai Y, Zorn AM, Yoshida H, Seldin MF, Nishikawa SI, et al. Mouse Wnt receptor gene Fzd5 is essential for yolk sac and placental angiogenesis. Development. 2001;128:25–33.
42. Davidson G, Wu W, Shen J, Bilic J, Fenger U, Stannek P, et al. Casein kinase 1 gamma couples Wnt receptor activation to cytoplasmic signal transduction. Nature. 2005;438:867–72.
43. Xu Q, Wang Y, Dabdoub A, Smallwood PM, Williams J, Woods C, et al. Vascular development in the retina and inner ear: Control by Norrin and Frizzled-4, a high-affinity ligand-receptor pair. Cell. 2004;116:883–95.
44. Landau DA, Tausch E, Taylor-Weiner AN, Stewart C, Reiter JG, Bahlo J, et al. Mutations driving CLL and their evolution in progression and relapse. Nature. 2015;526:525–30.
45. Rosati E, Sabatini R, Rampino G, De Falco F, Di Ianni M, Falzetti F, et al. Novel targets for endoplasmic reticulum stress-induced apoptosis in B-CLL. Blood. 2010;116:2713–23.
46. Baskar S, Ka YK, Hofer T, Levy JM, Kennedy MG, Lee E, et al. Unique cell surface expression of receptor tyrosine kinase ROR1 in human B-cell chronic lymphocytic leukemia. Clin Cancer Res. 2008;14:396–404.
47. Choi MY, Widhopf GF, Ghia EM, Kidwell RL, Hasan MK, Yu J, et al. Phase I Trial: Cirmtuzumab Inhibits ROR1 Signaling and Stemness Signatures in Patients with Chronic Lymphocytic Leukemia. Cell Stem Cell. 2018;22:951–9.
48. Fafilek B, Balek L, Bosakova MK, Varecha M, Nita A, Gregor T, et al. The inositol phosphatase SHIP2 enables sustained ERK activation downstream of FGF receptors by recruiting Src kinases. Sci Signal. 2018;11(548):eaap8608. https://doi.org/10.1126/scisignal.aap8608.
49. Gudernova I, Foldynova-Trantirkova S, El Ghannamova B, Fafilek B, Varecha M, Balek L, et al. One reporter for in-cell activity profiling of majority of protein kinase oncogenes. Elife. 2017;6:e21536. https://doi.org/10.7554/eLife.21536.
50. Dvorak P, Bednar D, Vanacek P, Balek L, Eiselleova L, Stepankova V, et al. Computer-assisted engineering of hyperstable fibroblast growth factor 2. Biotechnol Bioeng. 2018;115:850–62.
51. Harding HP, Novoa I, Zhang Y, Zeng H, Wek R, Schapira M, et al. Regulated translation initiation controls stress-induced gene expression in mammalian cells. Mol Cell. 2000;6:1099–108.
52. Yoon YM, Lee JH, Yun SP, Han YS, Yun CW, Lee HJ, et al. Tauroursodeoxycholic acid reduces ER stress by regulating of Akt-dependent cellular prion protein. Sci Rep. 2016;6:39838. https://doi.org/10.1038/srep39838.
53. Haugsten EM, Sørensen V, Brech A, Olsnes S, Wesche J. Different intracellular trafficking of FGF1 endocytosed by the four homologous FGF receptors. J Cell Sci. 2005;118:3869–81.
54. Zakrzewska M, Haugsten EM, Nadratowska-Wesolowska B, Oppelt A, Hausott B, Jin Y, et al. ERK-mediated phosphorylation of fibroblast growth factor receptor 1 on Ser777 inhibits signaling. Sci Signal. 2013;12;6(262):ra11. https://doi.org/10.1126/scisignal.2003087
55. Haugsten EM, Zakrzewska M, Brech A, Pust S, Olsnes S, Sandvig K, et al. Clathrin- and dynamin-independent endocytosis of FGFR3–implications for signalling. PLoS ONE. 2011;6(7):e21708. https://doi.org/10.1371/journal.pone.0021708.
56. Annamalai B, Liu X, Gopal U, Isaacs JS. Hsp90 is an essential regulator of EphA2 receptor stability and signaling: Implications for cancer cell migration and metastasis. Mol Cancer Res. 2009;7:1021–32.
57. Ou W Bin, Hubert C, Corson JM, Bueno R, Flynn DL, Sugarbaker DJ, et al. Targeted inhibition of multiple receptor tyrosine kinases in mesothelioma. Neoplasia. 2011;13:12–22
58. Laederich MB, Degnin CR, Lunstrum GP, Holden P, Horton WA. Fibroblast Growth Factor Receptor 3 (FGFR3) is a strong Heat shock protein 90 (Hsp90) client: Implications for therapeutic manipulation. J Biol Chem. 2011;286:19597–604.

59. Tang CHA, Ranatunga S, Kriss CL, Cubitt CL, Tao J, Pinilla-Ibarz JA, et al. Inhibition of ER stress-associated IRE-1/XBP-1 pathway reduces leukemic cell survival. J Clin Investig. 2014;124:2585–98.
60. Matsuo K, Machida H, Frimer M, Marcus JZ, Pejovic T, Roman LD, et al. Prognosis of women with stage I endometrioid endometrial cancer and synchronous stage I endometrioid ovarian cancer. Gynecol Oncol. 2017;147:558–64.
61. Lhomond S, Avril T, Dejeans N, Voutetakis K, Doultsinos D, McMahon M, et al. Dual IRE1 RNase functions dictate glioblastoma development. EMBO Mol Med. 2018;15(2): e16731. https://doi.org/10.15252/emmm.202216731.
62. Lee AH, Iwakoshi NN, Anderson KC, Glimcher LH. Proteasome inhibitors disrupt the unfolded protein response in myeloma cells. Proc Natl Acad Sci U S A. 2003;100:9946–51.
63. Dalton LE, Clarke HJ, Knight J, Lawson MH, Wason J, Lomas DA, et al. The endoplasmic reticulum stress marker CHOP predicts survival in malignant mesothelioma. Br J Cancer. 2013;108:1340–7.
64. Chen X, Iliopoulos D, Zhang Q, Tang Q, Greenblatt MB, Hatziapostolou M, et al. XBP1 promotes triple-negative breast cancer by controlling the HIF1α pathway. Nature. 2014;508:103–7.
65. Kaucká M, Krejčí P, Plevová K, Pavlová Š, Procházková J, Janovská P, et al. Post-translational modifications regulate signalling by Ror1. Acta Physiol. 2011;203:351–62.
66. McKenzie J, Smith C, Karuppaiah K, Langberg J, Silva MJ, Ornitz DM. Osteocyte Death and Bone Overgrowth in Mice Lacking Fibroblast Growth Factor Receptors 1 and 2 in Mature Osteoblasts and Osteocytes. J Bone Miner Res. 2019;34:1660–75.
67. Roschger P, Fratzl-Zelman N, Misof BM, Glorieux FH, Klaushofer K, Rauch F. Evidence that abnormal high bone mineralization in growing children with osteogenesis imperfecta is not associated with specific collagen mutations. Calcif Tissue Int. 2008;82:263–70.
68. Forlino A, Marini JC. Osteogenesis imperfecta. Lancet. 2016;387(10028):1657–71.
69. Houschyar KS, Tapking C, Borrelli MR, Popp D, Duscher D, Maan ZN, et al. Wnt Pathway in Bone Repair and Regeneration - What Do We Know So Far. Front Cell Dev Biol. 2019;6:170. https://doi.org/10.3389/fcell.2018.00170.
70. Laine CM, Joeng KS, Campeau PM, Kiviranta R, Tarkkonen K, Grover M, et al. WNT1 mutations in early-onset osteoporosis and osteogenesis imperfecta. N Engl J Med. 2013;368:1809–16.
71. Gong Y, Slee RB, Fukai N, Rawadi G, Roman-Roman S, Reginato AM, et al. LDL receptor-related protein 5 (LRP5) affects bone accrual and eye development. Cell. 2001;107:513–23.
72. Kalajzic I, Terzic J, Rumboldt Z, Mack K, Naprta A, Ledgard F, et al. Osteoblastic response to the defective matrix in the osteogenesis imperfecta murine (oim) mouse. Endocrinology. 2002;143:1594–601.
73. Gioia R, Panaroni C, Besio R, Palladini G, Merlini G, Giansanti V, et al. Impaired osteoblastogenesis in a murine model of dominant osteogenesis imperfecta: a new target for osteogenesis imperfecta pharmacological therapy. Stem Cells. 2012;30:1465–76.
74. Lombardi G, Di Somma C, Rubino M, Faggiano A, Vuolo L, Guerra E, et al. The roles of parathyroid hormone in bone remodeling: prospects for novel therapeutics. J Endocrinol Invest. 2011;34:18–22.
75. Kimura T, Bosakova M, Nonaka Y, Hruba E, Yasuda K, Futakawa S, et al. An RNA aptamer restores defective bone growth in FGFR3-related skeletal dysplasia in mice. Sci Transl Med. 2021;13(592):eaba4226. https://doi.org/10.1126/scitranslmed.aba4226.
76. Mossine VV, Waters JK, Hannink M, Mawhinney TP. PiggyBac transposon plus insulators overcome epigenetic silencing to provide for stable signaling pathway reporter cell lines. PLoS ONE. 2013;8(12):e85494. https://doi.org/10.1371/journal.pone.0085494.
77. Fafilek B, Hampl M, Ricankova N, Vesela I, Balek L, Kunova Bosakova M, et al. Statins do not inhibit the FGFR signaling in chondrocytes. Osteoarthritis Cartilage. 2017;25:1522–30.

Publisher's Note